The Astrophysical Journal Letters, 802:L26 (5pp), 2015 April 1 doi:10.1088/2041-8205/802/2/L26

THE ABSENCE OF AN ENVIRONMENTAL DEPENDENCE IN THE MASS–METALLICITY RELATION AT $z = 2$

Glenn G. Kacprzak[1], Tiantian Yuan[2], Themiya Nanayakkara[1], Chiaki Kobayashi[2,3], Kim-Vy H. Tran[4], Lisa J. Kewley[2], Karl Glazebrook[1], Lee Spitler[5,6], Philip Taylor[3], Michael Cowley[5,6], Ivo Labbe[7], Caroline Straatman[7], and Adam Tomczak[4]
[1] Swinburne University of Technology, Hawthorn, VIC 3122, Australia; gkacprzak@astro.swin.edu.au
[2] Research School of Astronomy and Astrophysics, The Australian National University, Cotter Road, Weston Creek, ACT 2611, Australia
[3] Centre for Astrophysics Research, Science and Technology Research Institute, University of Hertfordshire, Hertfordshire AL10 9AB, UK
[4] George P. and Cynthia Woods Mitchell Institute for Fundamental Physics and Astronomy, and Department of Physics and Astronomy, Texas A&M University, College Station, TX 77843-4242, USA
[5] Department of Physics and Astronomy, Macquarie University, Sydney, NSW 2109, Australia
[6] Australian Astronomical Observatories, P.O. Box 915, North Ryde, NSW 1670, Australia
[7] Leiden Observatory, Leiden University, P.O. Box 9513, NL-2300 RA Leiden, The Netherlands
Received 2015 February 19; accepted 2015 March 13; published 2015 April 2

ABSTRACT

We investigate the environmental dependence of the mass–metallicity relation at $z = 2$ with MOSFIRE/Keck as part of the ZFIRE survey. Here, we present the chemical abundance of a Virgo-like progenitor at $z = 2.095$ that has an established red sequence. We identified 43 cluster ($\langle z \rangle = 2.095 \pm 0.004$) and 74 field galaxies ($\langle z \rangle = 2.195 \pm 0.083$) for which we can measure metallicities. For the first time, we show that there is no discernible difference between the mass–metallicity relation of field and cluster galaxies to within 0.02 dex. Both our field and cluster galaxy mass–metallicity relations are consistent with recent field galaxy studies at $z \sim 2$. We present hydrodynamical simulations for which we derive mass–metallicity relations for field and cluster galaxies. We find at most a 0.1 dex offset toward more metal-rich simulated cluster galaxies. Our results from both simulations and observations suggest that environmental effects, if present, are small and are secondary to the ongoing inflow and outflow processes that are governed by galaxy halo mass.

Key words: cosmology: observations – galaxies: abundances – galaxies: evolution – galaxies: fundamental parameters – galaxies: high-redshift

1. INTRODUCTION

The evolution of galaxies is likely dependent on halo mass and regulated by baryonic feedback cycles (e.g., Dekel et al. 2009). In addition, environment plays a role in removing and truncating gas reservoirs while increasing the frequency of galaxy interactions/mergers, which could cause differences in morphology and color seen locally for field and cluster galaxies (e.g., Dressler 1980). However, selecting low-redshift galaxies by their stellar ages and stellar masses shows that their observable properties are independent of environment (see Blanton & Moustakas 2009 for a review). This is also confirmed by studies showing that the mass–metallicity relations of local field and cluster star-forming galaxies are consistent (Mouhcine et al. 2007; Ellison et al. 2009; Scudder et al. 2012; Hughes et al. 2013). If there is a difference in the mass–metallicity relation as a function of environment at $z \sim 0$, then it is observationally constrained to be around 0.05 dex (Ellison et al. 2009) while simulations constrain it to be less than ∼0.05 dex (Davé et al. 2011).

Although it is clear that a mass–metallicity relation exists at $z \sim 2$ (Erb et al. 2006; Sanders et al. 2014; Steidel et al. 2014), it is unclear if it differs as a function of environment at high redshift where clusters are beginning to form. Exploring the environmental influence on galaxies at high redshift is difficult since only a handful of spectroscopically confirmed clusters with $z \gtrsim 2$ exist (e.g., Kurk et al. 2004; Galametz et al. 2013; Gobat et al. 2013; Shimakawa et al. 2015; Valentino et al. 2015; Yuan et al. 2014). Only three studies have attempted to address the effects of environment on the mass–metallicity relation using small samples of galaxies or inhomgenous field and cluster selections and have produced conflicting results. A star-forming protocluster at $z = 1.99$ was found to be up to 0.25 dex poorer in metals (for six galaxies) than its field counterparts (Valentino et al. 2015), while two star-forming protoclusters at $z = 2.2$ (24 galaxies) and at $z = 2.5$ (36 galaxies) were found to be more enriched than those of field galaxies for $M_\star < 10^{11}$ $M_\odot$ (Shimakawa et al. 2015). On the other hand, Kulas et al. (2013) found for 20 star-forming protocluster galaxies that they do not exhibit a dependence of metallicity on mass (i.e., zero slope) with the low-mass protocluster galaxies showing an enhancement in metallicity compared to field galaxies. Although there appears to be some disagreement between studies, these ∼0.15 dex differences are marginally detected at less than 2σ.

Here, we present Keck/MOSFIRE observations from the ZFIRE survey[8] (T. Nanayakkara et al. 2015, in preparation) in order to clarify the debate on the dependence between the mass–metallicity relation and environment found at $z \sim 2$. We identified 43 cluster ($\langle z \rangle = 2.095 \pm 0.004$) and 74 field galaxies ($\langle z \rangle = 2.195 \pm 0.083$) (Spitler et al. 2012; Yuan et al. 2014) for which we can measure metallicities. This study is unique given the large number of galaxies obtained for a single cluster, with field galaxies selected the same way and observed simultaneously with the same instrument. In Section 2 we describe the data and our metallicity measurements. In Section 3 we present the mass–metallicity relation for field and cluster galaxies at $z \sim 2$. Our data are consistent with those of previously published field galaxy relations, however, contrary

[8] http://zfire.swinburne.edu.au

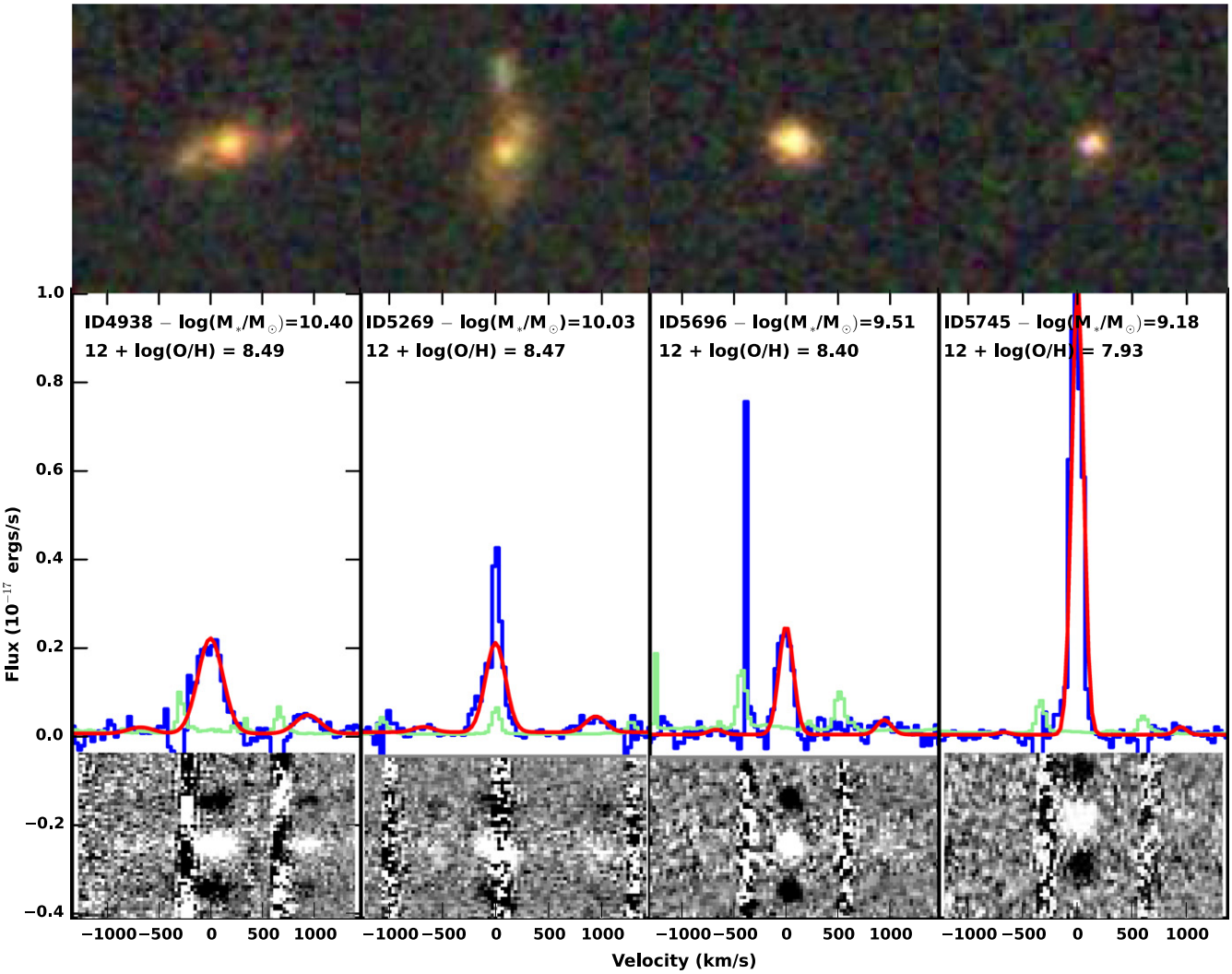

Figure 1. Representative sample of flux-calibrated 1D and 2D MOSFIRE spectra of four cluster members in order of decreasing stellar mass. The spectra are plotted with respect to the systemic velocity of each galaxy as definded by their nebular emission lines. Both the [N II] doublet and Hα are shown in the 1D and 2D spectra. Strong sky lines are seen as long vertical lines in the 2D spectra. The 1D data (blue), 1σ error spectra (green), and best-fit Gaussian models (red) are shown. The metallicity for each object is also listed. The top panels show 4″ × 4″ three-color *HST* images, using the F814W, F125W, and F160W filters, obtained from the publicly available CANDELS data (Grogin et al. 2011; Koekemoer et al. 2011; Skelton et al. 2014).

to other cluster galaxy works, we do not find a difference in the relation as a function of environment. We further show that this result is consistent with current simulation predictions. We end with concluding remarks in Section 4.

Throughout, we adopt a $h = 0.70$, $\Omega_{\rm M} = 0.3$, $\Omega_{\Lambda} = 0.7$ cosmology.

2. MOSFIRE SPECTROSCOPIC OBSERVATIONS AND SAMPLE

The $z = 2.095$ cluster was previously identified using the photometric redshifts (Spitler et al. 2012) from the medium-band Fourstar Galaxy Evolution Survey (ZFOURGE; C.M.S. Straatman et al. 2015, in preparation). As part of the spectroscopic follow up to ZFOURGE, the ZFIRE survey used Keck/MOSFIRE to spectroscopically confirm the existence of a Virgo-like progenitor at $z = 2.095$ containing at least 57 members with a velocity dispersion of 550 km s^{-1} (Yuan et al. 2014). Furthermore, the ZFIRE survey yielded an additional 123 spectroscopic redshifts of field galaxies with $1.98 \leqslant z \leqslant 3.26$. The spectroscopic targets were selected using the photometric redshifts from the K-band selected catalog from ZFOURGE (Spitler et al. 2014; C.M.S. Straatman et al. 2015, in preparation), which have an accuracy of $\Delta z/(1 + z_{\rm spec}) = 2\%$ (Tomczak et al. 2014; Yuan et al. 2014).

The MOSFIRE near-infrared K- and H-band spectroscopic observations, data reduction and flux calibration procedures are described in Yuan et al. (2014) with additional details to be presented in T. Nanayakkara et al. (2015, in preparation). All spectra are calibrated to vacuum wavelengths. Our typical 3σ flux limit is 1.8×10^{-18} ergs s^{-1} cm^{-2}.

Gaussian profiles were simultaneously fit to Hα and [N II] emission lines to determine their total flux. The line centers and velocity widths were tied together for a given pair of lines. Examples of our two-dimensional (2D) and one-dimensional (1D) MOSFIRE spectra and line fits are shown in Figure 1 for galaxies that have stellar masses ranging between $\log(M/M_{\odot}) = 10.4$–9.2 (also see Yuan et al. 2014 for additional examples).

We compute a gas-phase oxygen abundance for each galaxy using the N2 relation of Pettini & Pagel (2004) where 12 + log

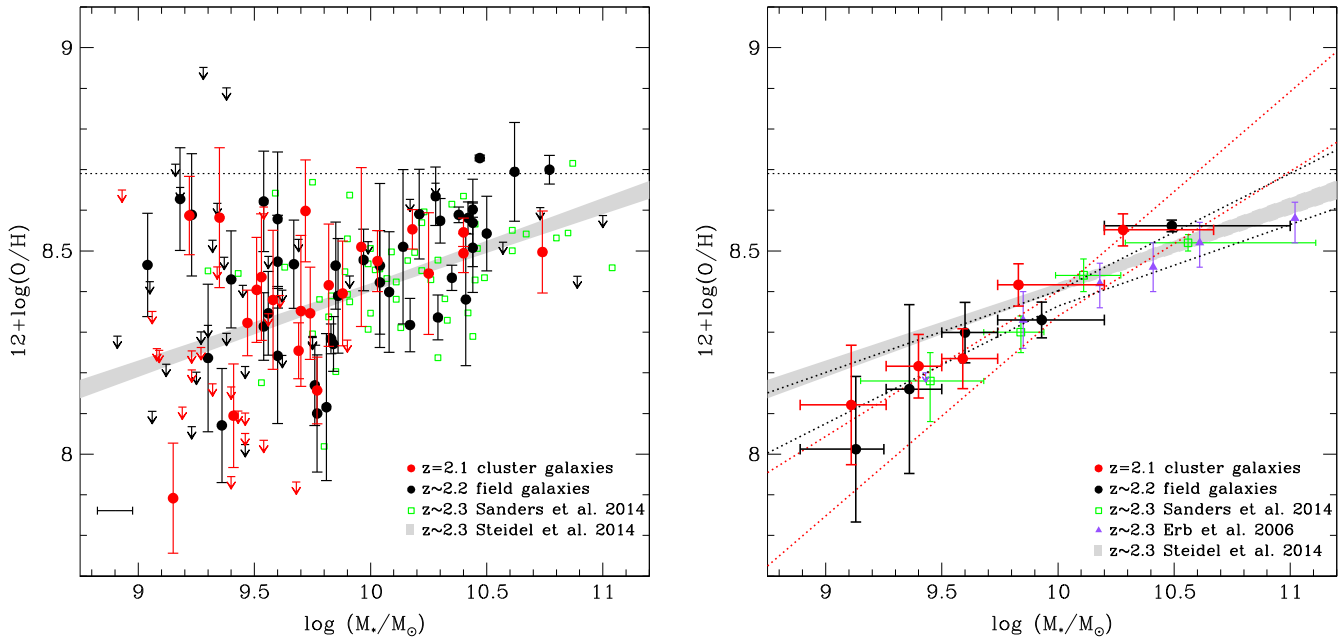

Figure 2. (Left) Mass–metallicity relation for star-forming $z = 2.1$ cluster (red) and $z \sim 2.1$ field galaxies (black). Circles indicate metallicity measurements where both Hα and [N II] are detected with greater than 3σ significance and downward arrows are quoted as 1σ limits on [N II]. The average error in determining the mass of galaxies using ZFOURGE photometry and FAST of $\pm$ 0.076 is shown in the bottom left. The green circles show the individual MOSDEF detections (Sanders et al. 2014), while the gray shaded region shows the fit to KBSS-MOSFIRE (Steidel et al. 2014). The dotted horizontal line is the solar abundance (Asplund et al. 2009).(Right) The dotted lines are bootstrap fits, with 1σ limits, to the mass–metallicity data from the left panel for cluster (red) and field (black) galaxies (see the text for details). The solid points are stacked spectra within a given mass bin and note that these are consistent with the fitted data. We further show additional binned data from the literature. Note both cluster and field galaxies are consistent within the 1σ errors.

(O/H) = 8.90 + 0.57 × N2 (N2 $\equiv$ log([N II]/Hα)). The Pettini & Pagel (2004) relation is established from a sample of low-redshift extragalactic H II regions for which both N_2 and oxygen abundances are directly measured. Applying this relation to high-redshift galaxies implies the caveat/assumption that the ionization parameters and electron densities are similar to those of low-redshift galaxies, however, it is known that typical ionization parameters are much higher for $z \sim 2$ galaxies with $\log(U) \geqslant 7.3$ (e.g., Shirazi et al. 2014; Steidel et al. 2014; Kewley et al. 2015). It is important to note, however, that Kewley et al. (2015) have shown that our $z \sim 2$ field and cluster galaxies have consistent ISM conditions, which allows for a meaningful direct comparison between the mass–metallicity relations of field and cluster galaxies.

From the parent sample of Yuan et al. (2014), we identify 49 cluster and 86 field galaxies with an Hα flux detected at greater than 3σ significance. Using the ZFOURGE active galactic nucleus (AGN) catalog (M. Cowley et al. 2015, in preparation), we remove AGNs from our sample (seven from the field, three from the cluster). An AGN is identified as either, or a combination of, an infrared source (following methods of Donley et al. 2012), an X-ray source (following methods of Szokoly et al. 2004), or a radio source (following methods of G. Rees et al. 2015, in preparation). In addition, we further require $\log([\mathrm{N\,II}]/\mathrm{H}\alpha) < -0.3$ (Sanders et al. 2014), which removes eight additional AGNs (five field, three cluster).

Our final sample contains 43 cluster ($\langle z \rangle = 2.095 \pm 0.004$) and 74 field galaxies ($1.98 \leqslant z \leqslant 2.56$, $\langle z \rangle = 2.195 \pm 0.083$) for which we can measure metallicities. We require a 3σ detection significance level for [N II]; otherwise 1σ detection limits are shown. Our final sample contains 22 metallicity measurements and 21 limits for the cluster galaxies and 41 metallicity measurements and 33 limits for the field galaxies.

We use stellar masses computed from the ZFOURGE photometry using Bruzual & Charlot (2003) stellar population models with FAST (Kriek et al. 2009), assuming exponentially declining star formation histories, solar metallicity, and a Chabrier (2003) initial mass function constrained to the spectroscopic redshift (see Tomczak et al. 2014 for details).

A 2D Kolmogorov–Smirnov test shows that the cluster and field galaxies have statistically consistent ($P(\mathrm{KS}) < 1\sigma$) observational properties such as extinction (determined by FAST) and star formation rates (determined by Hα—to be discussed in G. G. Kacprzak et al. 2015, in preparation).

3. RESULTS

3.1. ZFIRE Observations

In Figure 2 (left), we show the mass–metallicity relation for our field (black) and cluster (red) galaxies at $z \sim 2$, including 1σ limits. We have metallicity measurements for a significant range of galaxy masses from $8.9 \leqslant \log(M/M_\odot) \leqslant 11.0$. We further show the 53 individual detections from MOSDEF (Sanders et al. 2014) and the fitted relation from KBSS-MOSFIRE (Steidel et al. 2014). Note that the scatter in the data is similar to the scatter in the MOSDEF distribution and our data seem to follow the fitted data from KBSS-MOSFIRE. Furthermore, our cluster and field galaxies appear to have similar mass–metallicity distributions.

In Figure 2 (right), we show a bootstrap fit (1000 times) to the data from Figure 2 (left) using $12 + \log(\mathrm{O/H}) = y_i + m_i\,(M - 10)$. We fit the relation including the 1σ limits using the expectation–maximization maximum likelihood method of Wolynetz (1979). Including limits, we find for the cluster $y_c = 8.370 \pm 0.030$ and $m_c = 0.424 \pm 0.068$ while for the field we find $y_f = 8.384 \pm 0.018$ and

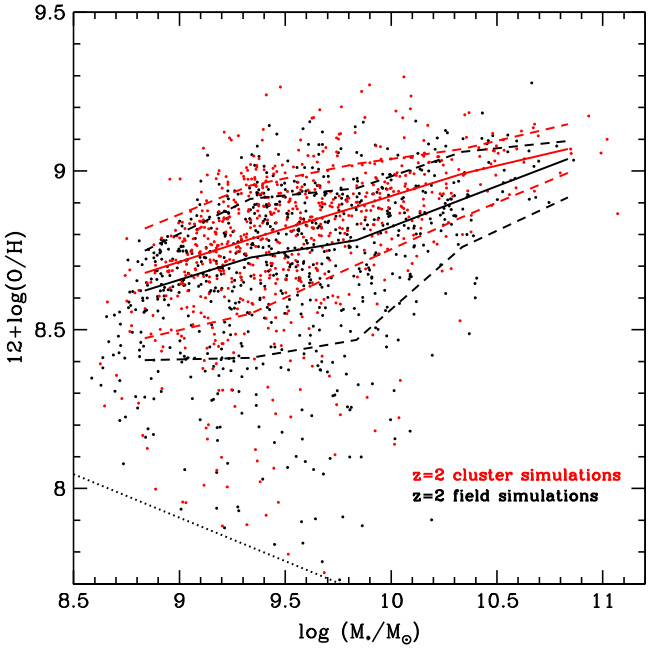

Figure 3. Mass–metallicity relation for simulated field (black) and cluster (red) galaxies. The solid and dashed lines show the moving median with a 68% confidence level. The dotted line is an observational limit of our ZFIRE survey (see the text for details). We find that both field and cluster galaxies have consistent mass–metallicity relations with maximum separations of 0.1 dex.

$m_f = 0.245 \pm 0.044$. These fits, along with their 1σ errors, are shown as dotted lines in Figure 2 (right). From the fitted data, we find that both cluster and field galaxies exhibit similar mass–metallicity relations and are consistent within 1σ. The maximum separation between the fitted field and cluster galaxy metallicity is at most 0.014 ± 0.035 dex. There could be a difference in the slope between field and cluster galaxies, which is mostly driven by the larger number of low-mass cluster metallicity limits.

To explore the similarities between the field and cluster galaxy data, we further stack the spectra in five mass bins with roughly equal numbers of galaxies per bin. We stacked the spectra, weighting by the uncertainty spectrum, to determine the typical metallicity in a given mass bin shown in Figure 2. We found no discernible difference if we weighted each spectrum by its Hα luminosity. Again, the stacked spectra show that cluster and field galaxies have equivalent mass–metallicity relations and are consistent within the 1σ errors. The stacked spectra are also consistent with the fits to the indvidual datapoints.

The fits and stacked data for both our field and cluster galaxies are consistent with the previous results of MOSDEF (Sanders et al. 2014), KBSS-MOSFIRE (Steidel et al. 2014) and Erb et al. (2006). However, the low-mass end of the field galaxies marginally deviates away from the KBSS-MOSFIRE fit, but is consistent with their binned data (not shown). Any observed minor differences could be due to sample selection biases (KBSS-MOSFIRE is rest-frame ultraviolet-selected while MOSDEF and ZFIRE are rest-frame optical-selected) or how detection significance levels and fits were conducted. However, the fact that our cluster and field data are consistent with those from all previous works further validates the lack of a difference between field and cluster galaxies.

3.2. Cosmological Simulations

To further examine if the environment of galaxies actually influences their metallicities, we perform a similar analysis using cosmological simulations. The simulations are performed with a Gadget-3-based hydrodynamical code that includes important baryon physics such as star formation, feedback from supernovae and AGNs, and chemical enrichment from Type II and Ia supernovae and asymptotic giant branch stars with a Kroupa IMF (see Kobayashi et al. 2007; Taylor & Kobayashi 2014 for details). Metallicities derived for the Kroupa IMF are virtually identical to those derived for a Chabrier IMF. The input nucleosynthesis yields are in excellent agreement with the observed elemental abundances in the Milky Way galaxy from carbon to zinc (Kobayashi & Nakasato 2011).

Different from the Davé et al. (2011) simulations, we include AGN feedback, whereby AGN-driven winds eject metals from massive galaxies to the intergalactic medium and some less massive galaxies undergo external enrichment depending on the environment. However, we find that for the mass–metallicity relation, the effect of AGNs is small and the trend originates mainly from supernova-driven/hypernova-driven galactic winds, which are much greater in less massive galaxies (Kobayashi et al. 2007).

The simulations are run for a $25\,h^{-1}$ Mpc box with two different initial conditions. The cluster simulation is chosen from 10 realizations to have the strongest central concentration, which gives the most massive galaxy with a stellar mass $\sim 10^{12}\,M_{\odot}$ (Taylor & Kobayashi 2014) at $z = 0$, while the field simulation is the same as that used in Kobayashi et al. (2007) and does not contain any central concentrations. The stellar masses are estimated by fitting a core-Sérsic profile, and the oxygen abundances are measured in $15\,h^{-1}$ kpc weighted by the star formation rates of gas particles to be comparable to our emission-line observations. At $z = 0$, the mass–metallicity relations of simulated galaxies are in good agreement with the observed mass–metallicity relations for both stellar and gas-phase metallicities (P. Taylor & C. Kobayashi 2015). These relations evolve as a function of time, with lower metallicities and a steeper slope at higher redshifts (Taylor & Kobayashi 2015, in preparation).

Figure 3 shows the mass–metallicity relations of the "cluster" and "field" simulations at $z = 2$. We apply an observationally based detection limit on the simulated mass–metallicity distribution. The N_2-based metallicity measurement is confined by the detection limit of [N II]. Based on a few simple assumptions, Yuan et al. (2013) used the SFR–mass relation, flux detection limit, and redshift to determine the observational detection limit on the mass–metallicity relation. For the ZFIRE survey, our typical 3σ flux limit is 1.8×10^{-18} ergs s^{-1} cm^{-2} resulting in the limiting relation of $12 + \log(\mathrm{O/H}) > -0.274 \times \log(M_{\star}/M_{\odot}) + 10.371$. This observational detection limit is important for understanding the incompleteness and biases due to observational limitations. While all of our observational data reside above this limit, we apply it to our simulated data (dotted line).

In Figure 3, the solid and dashed lines show the moving median with 68% confidence levels also shown. Both the field and cluster galaxies exhibit similar mass–metallicity relations within 1σ. The maximum separation between the fitted field and cluster galaxy metallicities is at most 0.1 dex. This is consistent with previous results from $z = 0$ simulations that

constrain the difference to be less than ∼0.05 dex (Davé et al. 2011).

Note that there is an ∼0.5 dex offset in the zeropoint between simulations and observations, which can be partly attributed to the uncertain normalization in metallicity measurements (e.g., Kewley & Ellison 2008; Davé et al. 2011).

4. CONCLUSIONS

High-redshift protoclusters are ideal laboratories in which to study the possible influences of the environment on galaxies. It is important to establish whether the environment can affect chemical evolution via restricting inflow and outflow, which may be responsible for galaxies migrating from the blue to the red sequence, or if a galaxy's chemical evolution is established early and is solely dependent on its internal evolutionary processes.

The environment may already be affecting the morphological properties of galaxies at $z = 2$. In our cluster, quiescent galaxies have similar colors and sizes relative to field quiescent galaxies, however, cluster star-forming galaxies are larger and redder on average when compared to field star-forming galaxies—suggesting environment can transform some galaxy properties at this early stage of formation (Allen et al. 2015).

It is a concern when searching for metallicity differences as a function of environment that the precise metallicities derived for high-redshift galaxies are likely incorrect due to their different ISM conditions relative to $z = 0$ galaxies—where emission-line metallicity indicators are calibrated (e.g., Pettini & Pagel 2004). However, this does not affect the relative offsets between the field and cluster galaxies given that Kewley et al. (2015) have shown that for our cluster, both field and cluster galaxies have similar ISM conditions.

Here, we present the chemical abundance of a Virgo-like progenitor at $z = 2.1$ (Yuan et al. 2014) which has an established red sequence (Spitler et al. 2012). Using our sample of field galaxies at a similar redshift, we show that the mass–metallicity relation of field and cluster galaxies is consistent with 1σ errors. We further show that both our field and cluster galaxies have consistent mass–metallicity relations when compared to other field galaxy surveys at $z \sim 2$ (Erb et al. 2006; Sanders et al. 2014; Steidel et al. 2014). Although we cannot rule out weak environmental trends in chemical enrichment, our analysis shows that the difference between field and cluster galaxies in the mass–metallicity relation is less than 0.02 dex.

Our simulations have shown that cluster galaxies may be marginally more metal-rich than field galaxies by at most 0.1 dex (although consistent within the scatter). This could be due to the removal of gas from the outskirts of galaxies which can produce an observed increase in metallicity by ∼0.1 dex (Hughes et al. 2013) or due to the shorter gas recycling times in denser environments (Oppenheimer & Davé 2008). However, given that the offset is small, it is suggestive that these effects do not play a significant role in the chemical evolution of galaxies, especially given that there is no observed differences in the mass–metallicity relation of field and cluster galaxies at $z = 0$ (Mouhcine et al. 2007; Scudder et al. 2012; Hughes et al. 2013).

Our results from the simulations and observations suggest that environmental effects, if present, are secondary to the ongoing internal processes within $z \sim 2$ galaxies that are likely governed by halo mass.

We thank Ryan Sanders and Alice Shapley for providing MOSDEF survey data. We thank Jackson Cunningham for his contributions during the initial stages of this project. G.G.K. was supported by an Australian Research Council Future Fellowship FT140100933. C. K. thanks the RSAA distinguished visitor program. K.G. acknowledges support from DP130101460 and DP130101667. Data was obtained at the W. M. Keck Observatory, which is operated as a scientific partnership among the California Institute of Technology, the University of California, and the National Aeronautics and Space Administration. The Observatory was made possible by the generous financial support of the W. M. Keck Foundation. Observations were supported by Swinburne Keck programs 2013B_W160M and 2014A_W168M and ANU Keck programs 20132B_WZ295M and 2014A_Z225M. Part of this work was supported by a NASA Keck PI Data Award, administered by the NASA Exoplanet Science Institute. The authors wish to recognize and acknowledge the very significant cultural role and reverence that the summit of Mauna Kea has always had within the indigenous Hawaiian community. We are most fortunate to have the opportunity to conduct observations from this mountain.

Facilities: Keck:I (MOSFIRE).

REFERENCES

Allen, R. J., Kacprzak, G. G., Spitler, L. R., et al. 2015, ApJ, submitted
Asplund, M., Grevesse, N., Sauval, A. J., & Scott, P. 2009, ARA&A, 47, 481
Blanton, M. R., & Moustakas, J. 2009, ARA&A, 47, 159
Bruzual, G., & Charlot, S. 2003, MNRAS, 344, 1000
Chabrier, G. 2003, PASP, 115, 763
Davé, R., Finlator, K., & Oppenheimer, B. D. 2011, MNRAS, 416, 1354
Dekel, A., Birnboim, Y., Engel, G., et al. 2009, Natur, 457, 451
Donley, J. L., Koekemoer, A. M., Brusa, M., et al. 2012, ApJ, 748, 142
Dressler, A. 1980, ApJ, 236, 351
Ellison, S. L., Simard, L., Cowan, N. B., et al. 2009, MNRAS, 396, 1257
Erb, D. K., Shapley, A. E., Pettini, M., et al. 2006, ApJ, 644, 813
Galametz, A., Stern, D., Pentericci, L., et al. 2013, A&A, 559, AA2
Gobat, R., Strazzullo, V., Daddi, E., et al. 2013, ApJ, 776, 9
Grogin, N. A., Kocevski, D. D., Faber, S. M., et al. 2011, ApJS, 197, 35
Hughes, T. M., Cortese, L., Boselli, A., Gavazzi, G., & Davies, J. I. 2013, A&A, 550, AA115
Kewley, L. J., & Ellison, S. L. 2008, ApJ, 681, 1183
Kewley, L. J., Yuan, T., Nanayakkara, T., et al. 2015, submitted
Kobayashi, C., & Nakasato, N. 2011, ApJ, 729, 16
Kobayashi, C., Springel, V., & White, S. D. M. 2007, MNRAS, 376, 1465
Koekemoer, A. M., Faber, S. M., Ferguson, H. C., et al. 2011, ApJS, 197, 36
Kriek, M., van Dokkum, P. G., Labbé, I., et al. 2009, ApJ, 700, 221
Kulas, K. R., McLean, I. S., Shapley, A. E., et al. 2013, ApJ, 774, 130
Kurk, J. D., Pentericci, L., Overzier, R. A., Röttgering, H. J. A., & Miley, G. K. 2004, A&A, 428, 817
Mouhcine, M., Baldry, I. K., & Bamford, S. P. 2007, MNRAS, 382, 801
Oppenheimer, B. D., & Davé, R. 2008, MNRAS, 387, 577
Pettini, M., & Pagel, B. E. J. 2004, MNRAS, 348, L59
Sanders, R. L., Shapley, A. E., Kriek, M., et al. 2014, arXiv:1408.2521
Scudder, J. M., Ellison, S. L., & Mendel, J. T. 2012, MNRAS, 423, 2690
Shimakawa, R., Kodama, T., Tadaki, K.-i., et al. 2015, MNRAS, 448, 666
Shirazi, M., Brinchmann, J., & Rahmati, A. 2014, ApJ, 787, 120
Spitler, L. R., Labbé, I., Glazebrook, K., et al. 2012, ApJL, 748, LL21
Spitler, L. R., Straatman, C. M. S., Labbé, I., et al. 2014, ApJL, 787, L36
Skelton, R. E., Whitaker, K. E., Momcheva, I. G., et al. 2014, ApJS, 214, 24
Steidel, C. C., Rudie, G. C., Strom, A. L., et al. 2014, ApJ, 795, 165
Szokoly, G. P., Bergeron, J., Hasinger, G., et al. 2004, ApJS, 155, 271
Taylor, P., & Kobayashi, C. 2014, MNRAS, 442, 2751
Taylor, P., & Kobayashi, C. 2015, MNRAS, 448, 1835
Tomczak, A. R., Quadri, R. F., Tran, K.-V. H., et al. 2014, ApJ, 783, 85
Valentino, F., Daddi, E., Strazzullo, V., et al. 2015, ApJ, 801, 132
Wolynetz, M. S. 1979, J. R. Stat. Soc., 28, 195
Yuan, T.-T., Kewley, L. J., & Richard, J. 2013, ApJ, 763, 9
Yuan, T., Nanayakkara, T., Kacprzak, G. G., et al. 2014, ApJL, 795, L20